

Improving Mechanical Properties of the Fe/epoxy Composite with a Novel Room Temperature-Thermal Curing Process

Haoqing Yang^{1, a}, Bailiang Zhuang^{1, b}, Yongyue Liu^{2, c}, and Jingkun Li^{3, d *}

¹ Jiangsu Branch of China Academy of Machinery Science and Technology Group Co., Ltd., Jiangsu 213164, China;

² Technology Center, Ningbo Heli Technology Shareholding Co., Ltd., Ningbo 315700, China;

³ Hebei Key Laboratory of New Functional Materials, School of Material Science and Engineering, Hebei University of Technology, Tianjin 300401, China.

^a yanghq_camjs@163.com, ^b 13585317691@163.com, ^c yongyue_liu@sina.com, ^d tjjk_zy@126.com

Abstract. A novel room temperature-thermal curing process was proposed to fabricate the Fe/epoxy composite easily and rapidly. The effect of thermal curing on the microstructure and mechanical properties were investigated. The results show that the thermal curing leads to the coarsening of Fe phase and the dense of Fe/epoxy interface. The average diameter of Fe increased from 36.03 μm to 64.91 μm after thermal curing, leading to the microstructure evolved from the island shape to the quasi reticular structure. The voids in the Fe phase and cracks along the phase boundary in the Fe/epoxy composite disappeared under the effect of diffusion. The tensile strength increased from 13.14 MPa to 53.72MPa and the elongation increased from 5.86% to 8.18% after thermal curing, with the improvement of 308.8% and 39.6%, respectively. The combination of brittle fracture in Fe and the crack elongation along the interface of Fe/epoxy improve both the strength and the plasticity of the Fe/epoxy composite. The Fe grains sustain fine with average size of 0.49 μm , contains abundant low-angle grain boundary (LAGBs) and deformed grains, but the density of dislocation and the value of texture are extremely low.

Keywords: Fe/epoxy composite; microstructure; mechanical properties; EBSD.

1. Introduction

As one of the traditional manufacturing tool, the molds was widely recognized as “the mother of industry”, which have been applied in aeronautics, automotive and many other industries [1-3]. Before the mass production of the products, some samples should be manufactured and tested. Thus the rapid molds have been generally used to produce the tested samples [4].

Generally, the rapid molds were manufactured by steels, which are heavy and high-cost with a long production cycle [5, 6]. To realize lightweight of the rapid molds as well as shorten the research and development cycle, the metal/high polymer composites have been employed into the rapid molds [7-9]. Meanwhile, the metal/high polymer composites could obtain excellent comprehensive performance, e.g., corrosion resistance [10, 11], wear resistance [12], weld ability [8] and mechanical properties [13, 14].

The main methods to manufacture the metal/high polymer composites were depend on additive manufacturing [15-17]. Based on a large number of investigations, researchers have found that the Fe/epoxy composites have outstanding toughness, tensile modulus and wear resistance [18, 19]. However, the characteristic of additive manufacturing limited the production cycle and mass manufacturing of the rapid molds.

In this paper, a novel room temperature-thermal curing process was proposed based on the fast cast process of steel molds and the good solidify ability of epoxy [3, 20]. The Fe powder and epoxy were stirred homogenous and solidified at room temperature for 4 h followed by heating to 80 °C and hold for 4 h. The evolution of microstructure and mechanical properties of the Fe/epoxy composites during the room temperature-thermal curing process and the grain size, grain boundary distribution, geometrically necessary dislocation, recrystallization behavior and grain orientation

have been investigated. The work provides new insight into the manufacturing of the rapid molds, which has both fundamental and applied significance for metal/high polymer composites.

2. Experimental procedure

2.1 Raw materials and process of fabrication.

The raw material used in the study was industrial pure iron (Fe) powder with the average diameter of 30 μm and the commercial epoxy resin, respectively. The volume ratio between the Fe powder and the epoxy was set as 1:1 according to the preliminary research [18].

The Fe powder and the liquid epoxy were stirred evenly for 5 min followed by stewing for 10 min to remove the bubbles. The homogenous slurry was put into a container and solidified in room temperature for 4 h. Then the block of Fe/epoxy composite was put into a KSL-1100X-S heating furnace, holding for 4 h at 80 $^{\circ}\text{C}$. The sample after solidification in room temperature was set as the contrastive sample to clarify the effect of thermal curing.

2.2 Characterization.

The microstructure and related compositions of the Fe/epoxy composites obtained by room temperature and room-high temperature solidification were observed by using a JSM-6510A scanning electron microscope (SEM) equipped with an energy dispersive spectrometer (EDS). The tensile tests at room temperature were carried at a UTM5105GD universal mechanical testing machine to obtain the tensile strength, elongation of fracture and compression strength. The fracture surfaces were observed by the JSM-6510A SEM. Electron backscatter diffraction (EBSD) technique was employed to characterize the grain size, grain boundary distribution, geometrically necessary dislocation, recrystallization behavior and grain orientation of the Fe in the Fe/epoxy composite. The EBSD sample was cut from the Fe/epoxy composite obtained by the room temperature-thermal curing process and minimized the residue stress by vibration polishing. The EBSD analysis was carried out by using a JEOL JSM-7800F SEM at 20 kV. The Oxford Instruments Nordlys Nano EBSD system equipped with Channel 5 software was applied to analysis the EBSD data.

3. Results and discussion

Figs. 1a and 1b show the microstructure of the Fe/epoxy composites with and without thermal curing, respectively. It could be found that the isolated Fe phase located on the epoxy matrix with the island shape. While the Fe phase are coarsening and coupling after the thermal curing, illustrating the quasi reticular structure.

Figs. 1c and 1d are the enlarged view of Figs. 1a and 1b, which focus on the phase boundary between Fe and epoxy. It could be observed voids in the Fe phase and cracks along the phase boundary in the Fe/epoxy composite without thermal curing. Then the phase boundary closes together with the diffusion of the C and Fe elements, as shown in Fig. 1c.

Fig. 1e shows the EDS pattern of the area in yellow dashed line of Fig. 1c. The main elements near the phase boundary are Fe, C and some elements included in the industrial Fe powder. It clarified the metallurgical bond between Fe and epoxy. Fig. 1f shows the particle size of the Fe in the Fe/epoxy composite. It shows that the holistic coarsening of Fe phase after thermal curing, whose average diameter increased from 36.03 μm to 64.91 μm . Therefore, the thermal curing could lead to the coarsening of Fe phase and the dense of interface of Fe/epoxy.

Fig. 2a shows the tensile strength and elongation of the Fe/epoxy composites before and after the thermal curing. It illustrates that the tensile strength increased from 13.14 MPa to 53.72MPa and the elongation increased from 5.86% to 8.18%, with the improvement of 308.8% and 39.6%, respectively.

Fig. 2b shows the typical tensile curves of the Fe/epoxy composites and the Figs. 2c-2f illustrates the related fracture surfaces. Some sudden decrease could be observed in the tensile curve of the Fe/epoxy composite with thermal curing, as pointed by the yellow arrow in Fig. 2b. From in Figs. 2c and 2e, it could be observed a large number of voids in the fracture surfaces, while most of the fracture occurred along the interface of Fe/epoxy. Thus some surface of metals expose on the fracture surface. However, the brittle fracture occurred in Fe of the Fe/epoxy composite with thermal curing, and some cracks formed on the interface of Fe/epoxy, as shown in Figs. 2d and 2f. With combination of the brittle fracture in Fe and the crack elongation along the interface, both the strength and the plasticity are improved by the thermal curing [15].

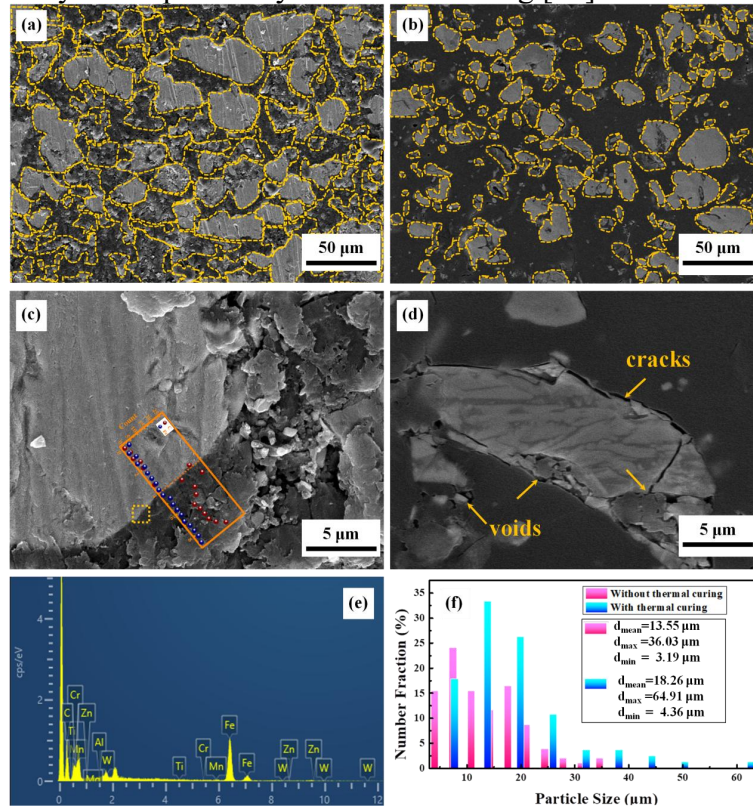


Fig. 1 Microstructure of the Fe/epoxy composites: (a) (b) are the SEM images of the Fe/epoxy composite with thermal curing and without thermal curing, respectively; (c) (d) are the enlarged images of (a) (b), respectively; (e) shows the EDS pattern of the area in the yellow dashed line of (c), and (d) is the distributions of the Fe particle size in the Fe/epoxy composites with and without thermal curing

Since the deformation of Fe plays a significant role in improving the mechanical properties of the Fe/epoxy. Further investigation of the Fe with thermal curing was carried out. The average grain size of Fe is $0.49 \mu\text{m}$ and 93.36% of the grains are finer than $1 \mu\text{m}$, as shown in Fig. 3a. It could be inferred that the thermal curing should not bring grain growth of Fe. A number of low-angle grain boundary (LAGBs) (2° - 15°) contained in the Fe, with number fraction of 87.03%, as shown in Fig. 3b. However, the average density of geometrically necessary dislocation in Fe is only $6.77 \times 10^{13} \text{ m}^{-2}$ (Fig. 3c), which is much lower in the metals [21]. The volume fraction of deformed grains in Fe is 65.35%, as shown in Fig. 3d. Thus the deformation degree and internal stress in Fe is low after the thermal process, although it contains a great number of deformed grains and LAGBs, which could play a positive role in improving both strength and plasticity of the Fe/epoxy composite.

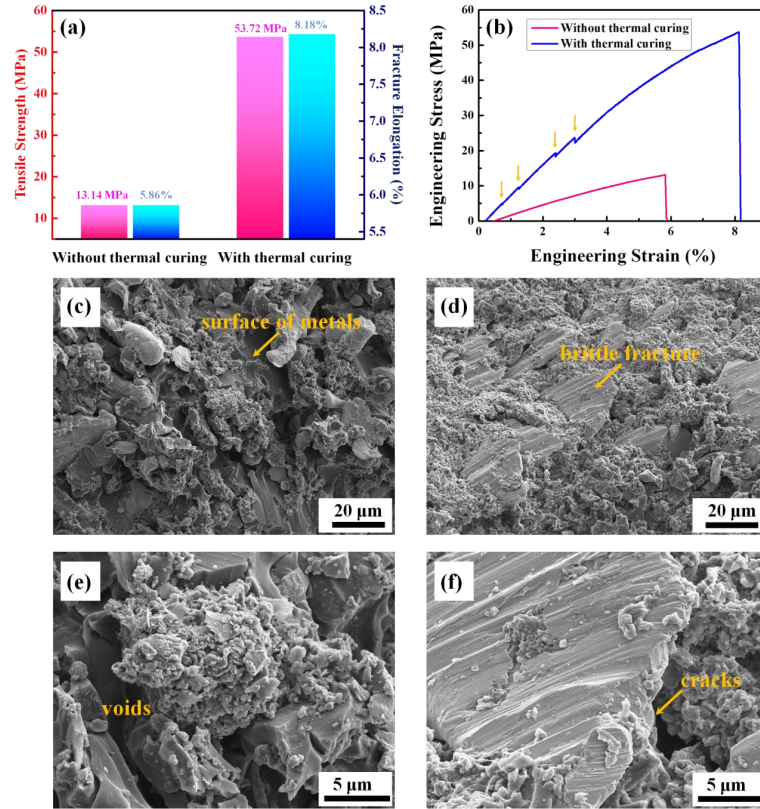


Fig. 2 Tensile properties of the Fe/epoxy composites: (a) shows the tensile strength and elongation; (b) illustrates the typical tensile curves; (c) (d) are the fracture surfaces after tensile of the Fe/epoxy composites before and after the thermal curing, respectively; (e) (f) are the enlarged images of (c) (d), respectively

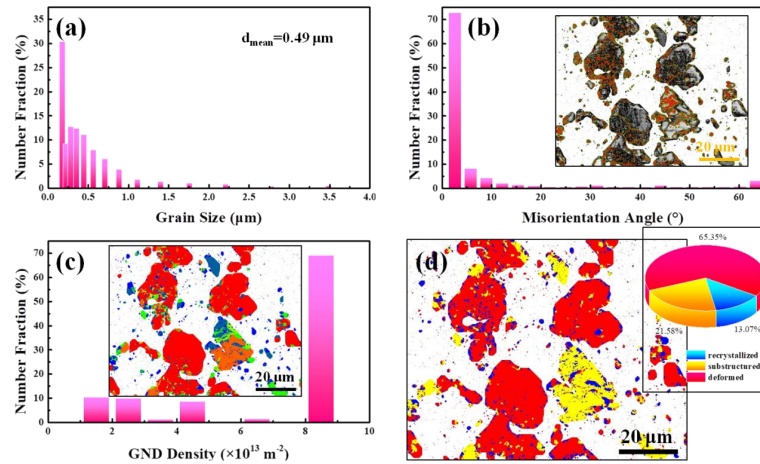


Fig. 3 Grain size distribution (a), misorientation distribution (with green line 2° - 15° and red line $> 15^\circ$) (b), GND density histogram (c), and recrystallization map (d) of the Fe in the Fe/epoxy composite fabricated by the room temperature-thermal curing process

Figs. 4a and 4b illustrate the orientation distribution function (ODF) plots for $\phi_2=0^\circ$ and 45° , respectively. In the body-centered cubic (bcc) metals, most of the deformed grains are rotated to the typical orientation as shown in Figs. 4 c and 4d [22]. The orientation of Fe in the Fe/epoxy composite is not the typical texture and the value is extremely low, which is beneficial to the coordinated deformation.

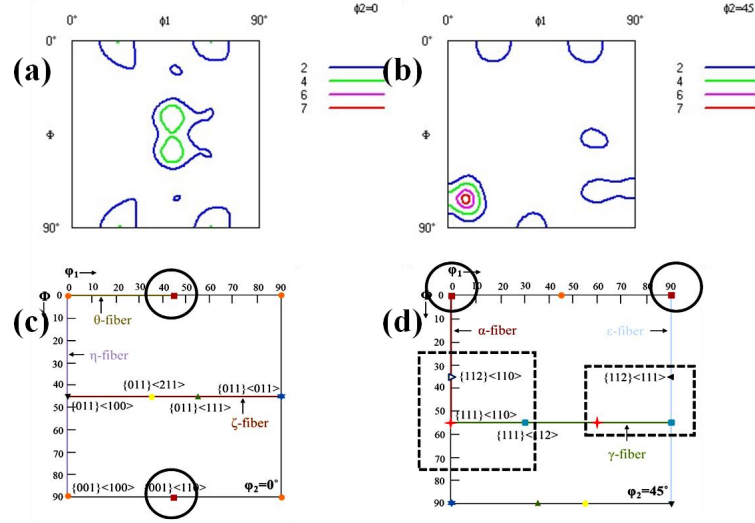


Fig. 4 ODF plots for $\phi_2=0^\circ$ (a) and 45° (b) for the of the Fe in the Fe/epoxy composite fabricated by the room temperature-thermal curing process, respectively; and the ideal $\phi_2=0^\circ$ (c) and 45° (d) texture components for bcc metals, respectively

4. Summary

In this study, a novel room temperature-thermal curing process was proposed to fabricate the Fe/epoxy composite easily and rapidly. The effect of thermal curing on the microstructure and mechanical properties of the Fe/epoxy composite as well as substructure and texture of the Fe were investigated. The following conclusions could be drawn:

(1) The thermal curing could lead to the coarsening of Fe phase and the dense of interface of Fe/epoxy. The average diameter of Fe increased from 36.03 μm to 64.91 μm after thermal curing, leading to the microstructure evolved from the island shape to the quasi reticular structure. While the voids in the Fe phase and cracks along the phase boundary in the Fe/epoxy composite disappeared under the effect of diffusion, forming the dense interface of Fe/epoxy.

(2) After the thermal curing, the tensile strength increased from 13.14 MPa to 53.72MPa and the elongation increased from 5.86% to 8.18%, with the improvement of 308.8% and 39.6%, respectively. The combination of brittle fracture in Fe and the crack elongation along the interface of Fe/epoxy improve both the strength and the plasticity of the Fe/epoxy composite.

(3) After the thermal curing, the average grain size of Fe is 0.49 μm and 93.36% of the grains are finer than 1 μm . The Fe in the Fe/epoxy composite contains abundant LAGBs and deformed grains, but the density of GNDs and the value of texture are extremely low.

Acknowledgements

This research was supported by the Jiangsu Provincial Science and Technology Plan Project (No. BK20211069) and the Ningbo Major Scientific and Technological Research and “Unveiling and Commanding” Project (No. 2022Z013).

References

- [1] Wen Wenxin, Li Luyao, Li Zheng, et al. Ultrasonic vibration-assisted multi-scale plastic forming of high-entropy alloys in milliseconds. *Rare Metals*, 2023, 42 (4): 1146-1153.
- [2] Yan Dandan, Shan Zhongde, Zang Yong, et al. Study on interlayer bonding properties of multi-material composite cast mold. *Materials Letters*, 2023, 335: 133750.

- [3] Xu Jingying, Kang Jinwu, Mao Weimin. Effect of double-layer-shell sand mold on the residual stress of casting and itself crack tendency. *Materials Letters*, 2023, 335: 133752.
- [4] Guo Zhengchuan, Xie Jun, Yang Jinghui, et al. Rapid mold temperature rising method for PEEK microcellular injection molding based on induction heating. *Journal of Materials Research and Technology*, 2023, 26: 3285-3300.
- [5] Ning Angang, Gao Rui, Yue Stephen, et al. Effects of cooling rate on the mechanical properties and precipitation behavior of carbides in H13 steel during quenching process. *Materials Research Express*, 2021, 8(1): 016503.
- [6] Makesh Kumar M, Anburaj J, Sasi Kumar M, et al. Effect of zirconium and niobium on the microstructure and mechanical properties of high-strength low-alloy cast steels. *Materials Research Express*, 2023, 10(5): 056506.
- [7] Badwe N, Mahajan R, Sieradzki K. Interfacial fracture strength and toughness of copper/epoxy-resin interfaces. *Acta Materialia*, 2022, 229: 117830.
- [8] Li Peiyong, Chen Li, Jiang Yanqing, et al. Large-area joining of CF/Epoxy skin and Al alloy web by an advanced continuous resistance spot welding technology to manufacturing wind turbine blade. *Materials Letters*, 2024, 356: 135614.
- [9] Lee H, Steven N. Adhesion of metallic glass and epoxy in composite-metal bonding. *Composites: Part B - Engineering*, 2018, 134: 186e192.
- [10] Wang Xinyue, Yang Zhou Dong, Wang Boya, et al. Effect of epoxy resin addition on properties and corrosion behavior of sintered joints in power modules serviced offshore. *Journal of Materials Research and Technology*, 2023, 25: 6593-6612.
- [11] Li Y, Deng Y G. Mechanical properties and corrosion resistance of high performance fiber-reinforced concrete with steel or amorphous alloy fibers. *Materials Research Express*, 2021, 8(9): 095201.
- [12] Zhang Jinglyen, Kong Gang, Li Shuao, et al. Graphene-reinforced epoxy powder coating to achieve high performance wear and corrosion resistance. *Journal of Materials Research and Technology*, 2022, 20: 4148-4160.
- [13] Zhou He, Tao Kun, Chen Bo, et al. Low-melting metal bonded MM' X/In composite with largely enhanced mechanical property and anisotropic negative thermal expansion. *Acta Materialia*, 2022, 229: 117830.
- [14] He Zhenhui, Tang Enling, Yao Wenjing, et al. Mechanical behavior and optimization of constitutive prediction model for Epoxy/Al energetic composite materials considering temperature and strain rate effects. *Journal of Materials Research and Technology*, 2023, 26: 2265-2281.
- [15] Masood S H, Song W Q. Development of new metal/polymer materials for rapid tooling using Fused deposition modeling. *Materials and Design*, 2004, 25: 587-594.
- [16] Zhang T, Padayodi E, Sagot J C, et al. Metallization of carbon-fibre reinforced composites via a metal-epoxy biphasic sublayer and low-pressure cold spraying. *Powder Technology*, 2023, 426: 118575.
- [17] Nikzad M, Masood S H, Sbarski I. Thermo-mechanical properties of a highly filled polymeric composites for fused deposition modeling. *Materials and Design*, 2011, 32: 3448-3456.
- [18] Singh R, Garg H, Singh S. Process capanality comparison of fused deposition modelling for ABS and Fe-nylon(6) feedstock filaments. *Materials Today Proceedings*, 2018, 5(2): 4258-4268.
- [19] Yu K C, Ma C C M, Teng C C, et al. Preparation and microwave absorbency of Fe/epoxy and FeNi3/epoxy composites. *Journal of Alloys and Compounds*, 2011, 509(33): 8427-8432.
- [20] Zarei F, Nuranian H, Shirvani K. In-situ formation of Al-alloyed surface layer on HH309 stainless steel by casting process. *Materials Research Express*, 2019, 6(9): 096573.
- [21] Xu Y, Toda H, Shimizu K, et al. Suppressed hydrogen embrittlement of high-strength Al alloys by Mn-rich intermetallic compound particles. *Acta Materialia*, 2022, 236: 118110.
- [22] Pal S, Alam M E, Maloy S A, et al. Texture evolution and microcracking mechanisms in as-extruded and cross-rolled conditions of a 14YWT nanostructured ferritic alloy. *Acta Materialia*, 2018, 152: 338-357.